Field studies of stable air flow over and around a ridge

Rowe, R.D. , Benjamin, S.F. , Chung, K.P. , Havlena, J.J. and Lee, C.Z.

FIELD STUDIES OF STABLE AIR FLOW OVER AND AROUND A RIDGE

R.D. Rowe, S.F. Benjamin*, K.P. Chung,
J.J. Havlena, and C.Z. Lee

Dept. of Chemical and Petroleum Engineering
The University of Calgary
Calgary, Alberta, Canada

* Present address: Advanced Projects Division, Leyland Cars,
550 Streetsbrook Road, Solihull, ENGLAND.

ABSTRACT

Three different field experimental techniques (smoke timelines, tetroon flights, and plume photography) have been used to examine the stable air flow field over and around a ridge. All of the data obtained from these field experiments are shown to be in good agreement with a two-layer model. It is also shown that the data obtained in the upper of the two layers, which flows over the terrain, fit well with a simple potential flow model. The ridge is reasonably two-dimensional with a length-to-width ratio of about 5. These field data for this fairly long ridge are found to be in much better agreement with laboratory data (available in the published literature) for axisymmetric hills rather than those for two-dimensional barriers with gaps.

1. INTRODUCTION

Atmospheric dispersion in an area of complex topography can be very different from and much more complicated than that over flat ground. The rapid increase of actual and potential industrial development in areas of complex topography is the principal motivation at this time for the development of improved prediction methods for air pollutant concentrations in this kind of an area. Egan (1975) has provided an excellent review of work pertinent to this problem up to the mid-nineteen-seventies. It is evident that much more work needs to be done to better understand the diffusion and transport of airborne material within rugged areas, and to provide some evidence to support or to suggest modifications to the various models currently in use. The stable atmospheric condition has been identified by many regulatory agencies as the worst case for rugged terrain, and horizontal trajectory models with effectively direct impaction on the terrain feature have been developed, e.g. the EPA Valley model (Burt and Slater, 1977). In this paper, three different field experiments (smoke timelines, tetroon flights, and plume photography) that have been used to examine the stable air flow field over and around a ridge are reported.

For stable atmospheric conditions, it is often observed that the lower air layer stagnates as cool 'pools' or alternatively this layer moves around rather than over a terrain feature; see, for example, Scorer (1968). A simple two-layer approach to model this type of behaviour, where only the upper layer moves over the terrain feature, has been used by a number of investigators (Sheppard, 1956; Drazin, 1961; Egan, 1975; Brighton, 1978; Snyder, Britter, and Hunt, 1979; Baines, 1979; Hunt and Snyder, 1980; Rowe, 1980). The essence of a two-layer model was given some 25 years ago by Sheppard (1956) when he attempted to answer the question: 'Under what conditions will an airstream rise over

a mountain range?'. Unfortunately, there does not appear to be a unique answer to this question which applies in all situations. For example, when inversion conditions exist for a significant portion of the troposphere, and lee waves could be produced downwind of a terrain obstacle, then the coupling that exists throughout the stable air flow can provide the additional energy required for low lying air parcels to surmount the terrain obstacle (Baines, 1977; Scorer, 1978). However, when negligible coupling exists, as is the case when neutral or unstable stratification overrides stable stratification, then it is believed that a two-layer model provides a good approximation for the flow field in the stable region. A typical nocturnal inversion is a good example of this situation; therefore, the two-layer approach can be applied on many occasions when a stable atmosphere is being advected towards a terrain obstacle.

For a perfectly two-dimensional terrain feature the lower layer may be completely blocked (see, for example, Baines, 1977 and 1979); however, a natural obstacle is never perfectly two-dimensional and the lower layer may flow around the ends. With this problem in mind, Brighton (1978) posed the question: 'Does the possibility of flow round the ends of even a very long obstacle allow this fluid to drain away leading to a flow qualitatively different from the two-dimensional one, or is there a continuous transition between the two?'. The field experiments reported here were performed in the vicinity of a reasonably two-dimensional ridge with a length-to-width ratio of about 5, and the data indicate that the lower layer flows around this fairly long obstacle.

Although the local heating or cooling of the surface of a terrain feature can induce anabatic or katabatic winds, and/or influence the flow separation (Scorer, 1968), which may be at least as significant as the advected flow, these effects are not evident in our field data.

Implications for stack design

If a stack is located close to much higher terrain feature, then for stable atmospheres the plume follows the lower layer flow. In support of horizontal trajectory models, such as the EPA Valley model, it should be noted that it is certainly possible for the plume in the lower layer to impact on the terrain feature if the stagnation streamline passes close to the location of the stack (Burt and Slater, 1977; Brighton, 1978). In this case, the plume is imbedded in flow around both sides of the obstacle; a theoretical model to describe this type of behaviour has been developed by Hunt, Puttock, and Snyder (1979). However, on most occasions when the wind direction takes the plume towards the terrain feature the plume flows with the streamlines around one side, and it does not normally contact the feature because of the slow rate spread of the plume by turbulent diffusion in a stable atmosphere.

If the plume height has about the same elevation as that of the terrain feature, as is the case in one of the experiments reported here, then the plume follows the upper layer flow over the topography. Because the diffusion of the plume about its centreline is small for this type of atmosphere, the plume may well clear the crest of the terrain feature completely, but it could still be brought down to the ground in the lee side flow (Hunt and Snyder, 1980). On the other hand, if the plume height is somewhat greater than the elevation of the terrain feature, then the plume will probably clear the lee waves behind the topography. In this situation, the more unstable neutral atmosphere which enables the pollutant to be diffused to the topography would probably be the worst case (Leahey and Rowe, 1974).

Interface elevation, H_d

If the elevation of the interface between the two layers H_d is determined by those air parcels which just have sufficient upstream kinetic energy to do the work of overcoming the opposing inversion buoyancy force and reach the crest of a terrain feature of height h, then it can easily be shown (see Appendix) that

$$H_d = h(1 - F) \tag{1}$$

when the Froude number F is less than one $(F < 1)$. When $F > 1$ all of the air flows over the terrain obstacle. Snyder, Britter, and Hunt (1979) found that the values of the H_d obtained in the laboratory for three different axisymmetric hill shapes in stably stratified flows are predicted almost exactly by equation (1). In agreement with the theory of Drazin (1961), they also found that the fluid in the lower layer is constrained to move in essentially horizontal planes round these obstacles. Our field data support these laboratory results. However, it must be noted that Baines (1979) has recently reported laboratory data for two-dimensional barriers with gaps which all reasonably well agree with the following simple but different equation

$$H_d = h(1 - 2F) \tag{2}$$

when $F < 0.5$, and the fluid in the lower layer flows around the barrier through the gap. All of the fluid flows over his obstacles when $F > 0.5$ (rather than $F > 1$ above). Baines (1979) also found the same results for the two-dimensional barriers without gaps, except that in this case the fluid in the lower layer is blocked.

Potential flow in upper layer

Hunt and Snyder (1980) have observed the flow structure over a three-dimensional bell-shaped hill of height h when it was placed first in a large towing tank containing stratified saline solutions with uniform stable density gradients and second in an unstratified wind tunnel. They have provided a plot of the distance n_s from the hill top to a streamline as a function of upwind streamline height H_s (figure 18 on page 696 of their paper). Rowe, Lee, and Havlena (1980) have replotted these data using the appropriate coordinates for the layer that flows over the hill, i.e. $n_s/(h - H_d)$ against $(H_s - H_d)/(h - H_d)$ where equation (1) was used to determine H_d, rather than the axes n_s/h versus H_s/h used by Hunt and Snyder. Only those data points with $F < 1$ had to be moved to take account of the new axes. It was found that there is still considerable scatter of the data points for $F < 1$, and thus the flow structure in the upper layer is evidently dependent on the Froude number. However, the curve through the $F = 1.0$ data does provide a reasonable average estimate for most of the $F \leq 1$ points. The elevations of the $F = 1.0$ data above the hill top have only about one half of the values predicted by potential flow theory; but, as shown by the $F = 1.6$ data points, the Froude number does not have to be much greater than one for the streamlines to approximate potential flow.

Although the laboratory data of Hunt and Snyder show that potential flow overestimates the elevation of streamlines above a hill top when $F \lesssim 2$, potential flow is able to account for gross terrain differences in a very simple manner, and can handle three-dimensional as well as two-dimensional flow situations. In this paper, the flow in the upper layer that passes over a ridge is compared to two-dimensional potential flow; the equations are provided in the Appendix.

2. EXPERIMENTAL SITE

The field program has been conducted in the vicinity of the Shell Jumping Pound sour gas processing plant, which is located in the foothills to the east of the Rocky Mountains. The major source of SO_2 at this plant is the sulphur recovery unit incinerator stack. A topographical map of the area is given in Fig. 1. The primary reason for the selection of this site is the existence of a long reasonably two-dimensional ridge, called the Copithorne Ridge. This ridge runs along the NNW-SSE direction and lies about 1 km east of the plant. The crest elevation is almost the same as that of the incinerator stack ($\simeq$ 100 m). Thus the location of the ridge is closer than the point of maximum ground level concentration expected for a flat terrain, and the ridge is significant enough to modify the air flow at stack height. The ridge shape is fairly well defined so that qualified generalizations to flows in similar cases can be made. The site is only about 30 minutes driving time from the University of Calgary, and is easily accessible from the Trans-Canada Highway.

There are three air pollution monitoring trailers in the vicinity of the gas processing plant. Two of them (NE and SE trailers) are located on top of the Copithorne Ridge and are separated by about 1.3 km. The NE trailer is located near the highest point on the Copithorne Ridge. The SE trailer is situated beside a gap in this ridge. The third trailer (NW trailer) is positioned on the side of the Crawford Plateau to the north of the plant. Each trailer houses pollutant measurement instruments and a continuous chart recorder for the wind speed and direction. The wind vane and cup-type anemometer at each trailer is mounted on a tower at 10 m above the ground.

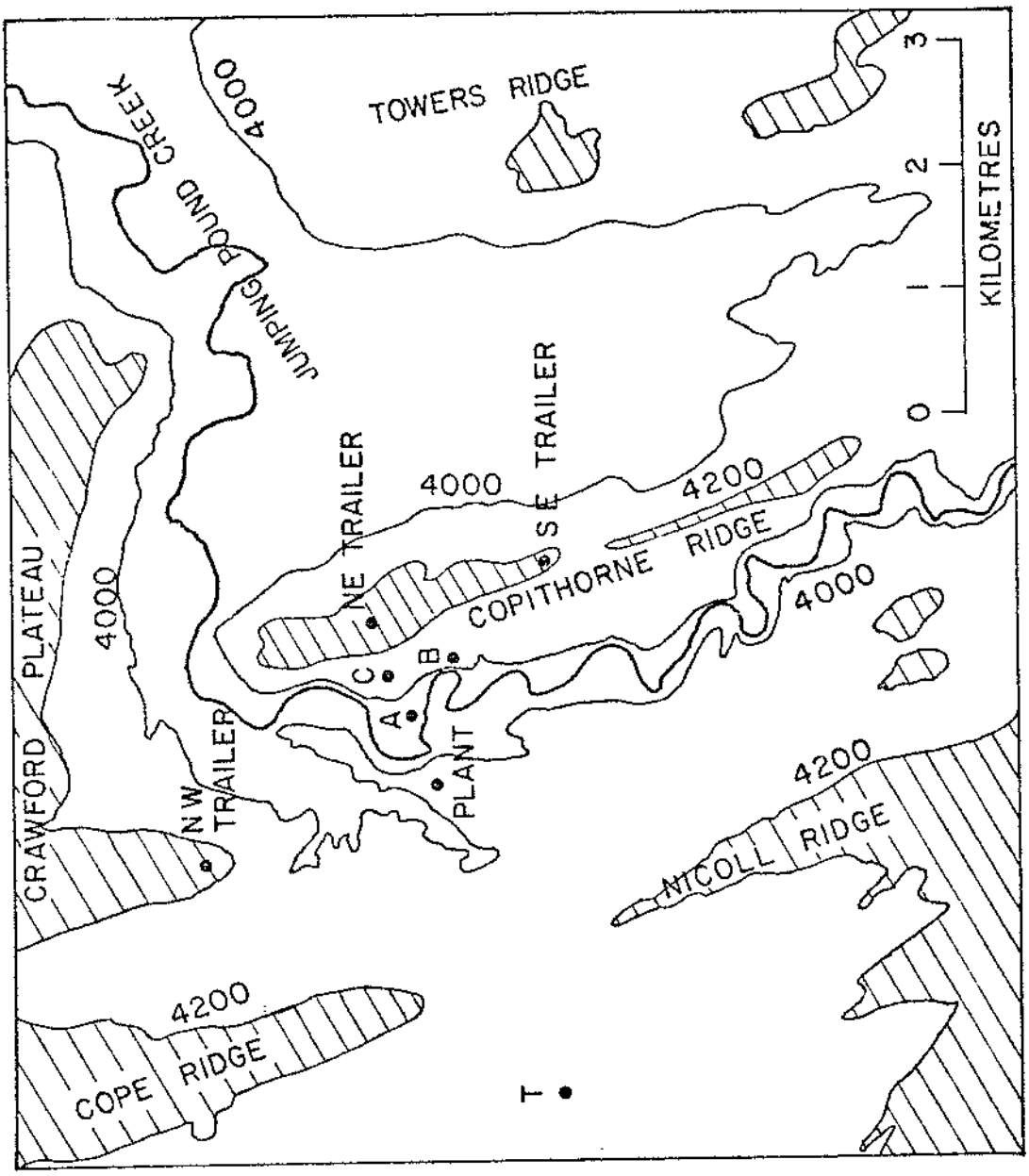

Fig. 1. Map of site. Elevation above 4200 feet ASL has been hatched to indicate the topography. The 4000 feet ASL contour line is also shown.

3. OTHER WORK AT THIS SITE

A number of field experiments have been conducted since 1972 to determine the extent to which the Copithorne Ridge affects the plume dispersion, air flow, and air quality. Helicopter-borne SO_2 measurements in the incinerator stack plume as it passed over the ridge were made in November 1972 (Leahey and Rowe, 1974). It was deduced from these data that the neutral stability atmosphere streamlines do not approach the ridge quite as closely as those predicted by simple potential flow theory. The potential flow approach was therefore used as a conservative design criterion to determine the required height of a new incinerator stack. A new 102.1 m (335 ft) stack was commissioned in November 1974; the old stack was 68.6 m (225 ft) high.

A detailed analysis of the wind and SO_2 data collected at the two trailers on the Copithorne Ridge for two two-year periods has been reported by Benjamin and Rowe (1979). One of the two-year periods covers emissions from the old incinerator stack and the other two-year period is for the new incinerator stack. The results show that there are a variety of weather types producing peak concentrations at each trailer; a "peak" concentration is defined as any concentration greater than 0.1 ppm. The weather types providing the highest sum total duration of peak concentrations are the light wind stable and the windy neutral atmospheres. Increasing the incinerator stack height reduced the frequency of occurence of peaks at the NE trailer by about 50% irrespective of weather type with the exception of the summer convective atmosphere.

A series of tetroon flights were performed in the daytime during the summer of 1977 (Benjamin, Havlena, and Rowe, 1978). Large instabilities

were observed during windy neutral atmospheric conditions as well as on days with strong thermal convection. The instabilities extended to several hundred metres above the ground, and were an order of magnitude greater than the height variations of the underlying terrain (Fig. 1). Under more stable conditions the air flow was observed to reflect the structure of the terrain more closely.

The three experimental techniques that have been used to examine the flow over and around the Copithorne Ridge for stable atmospheres are reported in the next three sections.

4. SMOKE TIMELINES

A smoke timeline flow visualization technique was used in the summer of 1976 to study the air motion in stable atmospheres around the ridge. The method involved fixing an orange smoke generator to a helium filled balloon, activating the generator at the ground and releasing the balloon. The smoke was generated continuously for about one minute as the balloon rose leaving an almost vertical smoke trail up to 200 m above the release point. Two cine cameras photographed the smoke simultaneously, enabling the trajectories of selected smoke elements to be found. The cameras were positioned at points A and B and the balloons were released at position C in Fig. 1.

A photogrammetric technique has been developed from which the trajectory of a smoke element can be found (Benjamin, 1976). A smoke element common to both cameras is located and its history followed on both films. This necessitates synchronization of the two cameras and this was achieved by observing a common event on both films and knowing the filming speeds.

The initial position of a chosen smoke element was obtained by observing that smoke puff directly under the balloon on the two synchronized films, i.e. the smoke puff last generated. This element was then followed for the same period on both films. This technique provides a detailed picture of the vertical wind profile, but it can only be used for stable flows because the smoke disperses too rapidly in other types of atmospheres.

The best quantitative example took place early on the morning of July 16; three smoke trails were photographed between the hours 7:33 to 8:03 MDT. A deep radiation inversion, 280 m in extent, had formed overnight and the flow was towards the ridge. The initial positions of the smoke elements chosen for analysis in relation to the terrain slope are shown in Fig. 2. The vertical scale has been exaggerated for clarity and the terrain cross-section is that following the mean path of the rising smoke generator/balloon package. The lapse rate, obtained from a minisonde released at 06:30 MDT, is also shown. It can be seen that the value of this ambient lapse rate Λ lies between -2 and -4 °C/100 m. Fig. 3 shows the wind direction profiles as functions of height above the balloon release point. The zero degree reference direction has been taken along the crest of the ridge; the flow was approximately NW.

The wind directional shear close to the release point decreases systematically for each subsequent ascent later in time. Particular attention should be given to the lowest two points X_1 and Y_1 for the first ascent. A wind directional shear of 40° occurs between these two points which are separated by only 14 m in the vertical direction. The flow for the lowest point X_1 is almost parallel to the ridge crest. It appears that the interface between the two layers lies between X_1 and

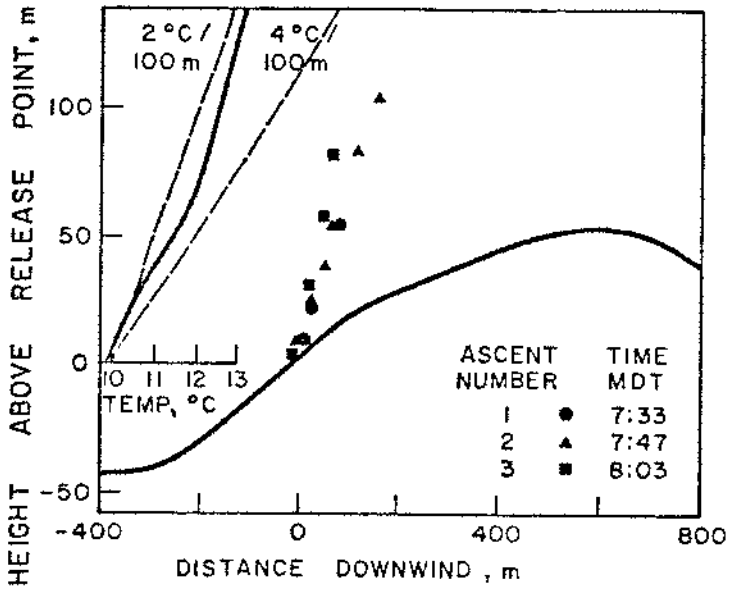

Fig. 2. The initial positions of smoke elements that were followed to obtain the velocity profiles. The vertical temperature gradient is also shown.

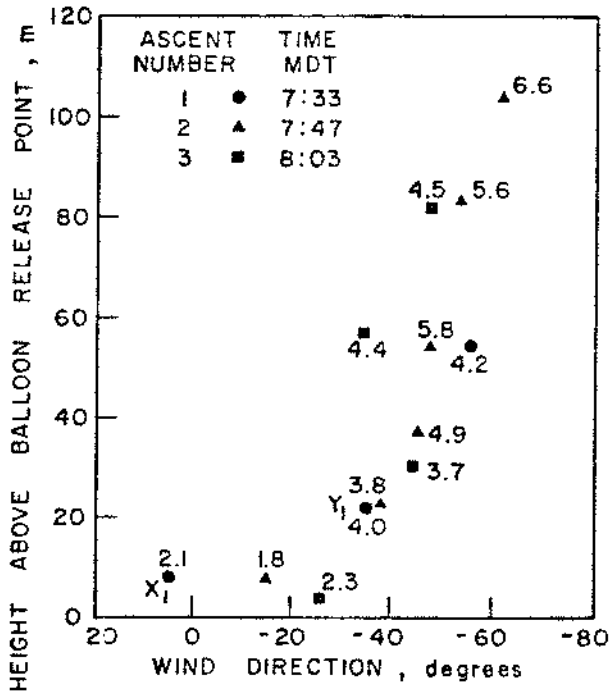

Fig. 3. Wind direction profiles for three ascents. The zero degree reference line lies along the ridge crest with negative values for flow towards the ridge. The numbers adjacent to the symbols give wind speed, m/s.

Y_1; X_1 is located approximately 50 m below the ridge crest. This proposition is in reasonable agreement with equation (1), as can be seen by comparing the values tabulated in Table 1 with equation (A6) in the Appendix. A much stronger inversion is required for equation (2) to apply. By the time of the second and third ascents, the strength of the inversion had decreased sufficiently to have either pushed the interface between the two layers below the balloon release point or alternatively to have eliminated the lowest layer altogether.

Table 1. Atmospheric parameters for smoke timelines

Lapse rate, Λ (°C/100 m)	(Brunt-Vaisala frequency, N)$^{-1}$ (s)	$\frac{U}{N}$ (m)	Froude number, F
-2	31	65	0.67
-4	24	50	0.52

The ambient temperature T_o = 10°C, the wind speed (at X_1) U = 2.1 m/s, and the Froude number F = U/(Nh), where the ridge crest elevation h = 97 m.

5. TETROON FLIGHTS

A series of tetroon flights were conducted on clear nights, when stable atmospheric conditions prevail (Chung, 1979). All but one of these flights were made during the summer of 1978, the additional case was obtained from the daytime flights during the previous summer (Benjamin, Havlena, and Rowe, 1978). A flashing light device was attached to each nighttime tetroon so that it could be tracked by two theodolites, which were located next to the NE and SE trailers on the Copithorne Ridge. The tetroons were released

near point T (Fig. 1) about 4 km upwind of the ridge, in order that they could level off over reasonably flat terrain. All of the tetroons were ballasted to float at an equilibrium level of 100 m above the ground.

Nine tetroons flew across the ridge in directions that were approximately normal to its crest line. All of these 9 tetroons followed almost straight paths passing over the ridge close to the SE trailer. The ridge cross-section is reasonably symmetrical and its aspect ratio L/h in the vicinity of the SE trailer has a value of approximately 4.5 (L is half of the length between the half-height positions, see Fig. A1).

Minisondes were released to determine the lapse rate A. Unfortunately, it was not normally possible to determine the lapse rate from these data more accurately than to the nearest degree Celsius per 100 m. The mean wind speed U could be found from the tetroon flight data to the nearest metre per second. Thus, the natural air wavelength $2\pi U/N$ (where N is the Brunt-Vaisala frequency, see Appendix) could only be estimated to the nearest half kilometre. These parameters for each of the 9 flights are given in Table 2.

It can be seen from Table 2 that the 9 tetroon flights can be split into two sets. The natural air wavelengths are about 3 and 1.5 km for flights A-E and F-I respectively, i.e. twice as large and the same as the total base width ($\simeq 6L$) of approximately 1.5 km for the Copithorne Ridge. The Froude numbers $F = U/(Nh)$ are about 8 and 4 for the ridge elevation near the SE trailer ($h \simeq 60$ m) for flights A-E and F-I respectively.

The tetroon trajectories are shown in Fig. 4; flights A-E are denoted by solid lines, whereas flights F-I are given by dashed lines. It is not

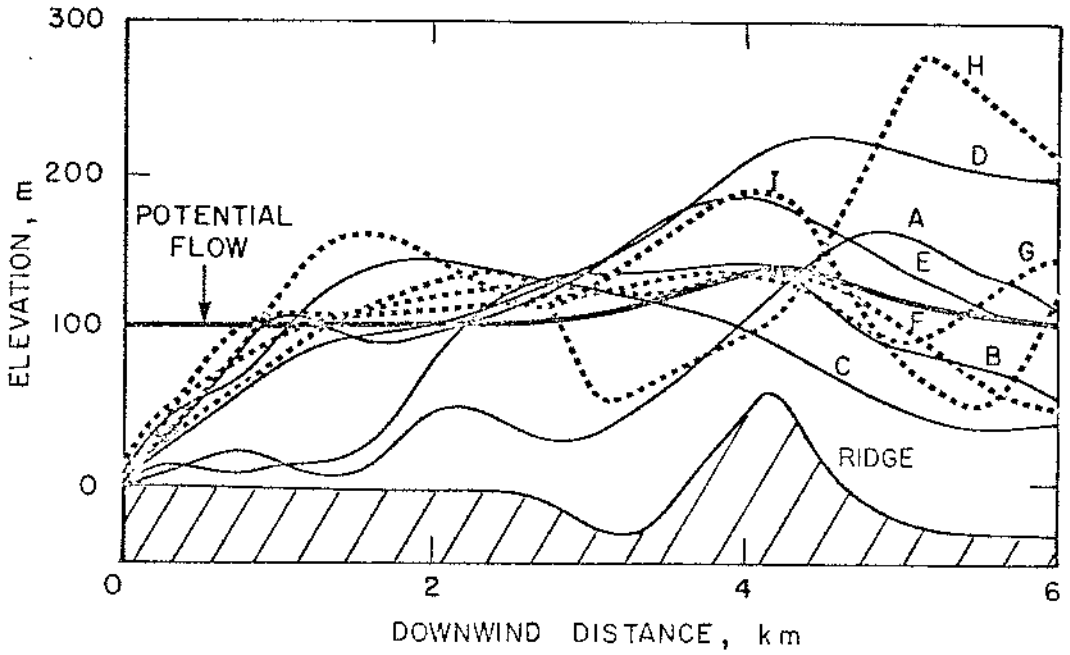

Fig. 4. Tetroon trajectories across the ridge.

possible to discern any systematic difference between the two sets of tetroon flights. All of the trajectories are on the average in reasonable agreement with the single layer potential flow streamline whose upwind elevation is 100 m.

Table 2. Tetroon flight parameters

Tetroon	Date	Release time MDT	Lapse rate, Λ (°C/100 m)	Wind speed, U (m/s)	Natural air wavelength, $2\pi U/N$ (m)
A	20-9-77	0930	0	10	3000
B	11-7-78	2140	0	8	2500
C	12-7-78	0220	-1	12	3000
D	12-7-78	0540	-2	14	3000
E	12-7-78	0640	-1	12	3000
F	19-6-78	0100	-2	8	1500
G	19-6-78	0630	-3	8	1500
H	19-6-78	0800	-2	5	1000
I	19-7-78	0630	-2	8	1500

6. PLUME PHOTOGRAPHY

Time lapse photographs of the plume from the cooling tower at the gas plant were taken during the two winters of 1978 and 1979. The cooling tower is of the mechanical draft type with two small stacks on the top of the frame, the total height of the unit is 11.2 m. The photographs were taken from the NW trailer, which is located to the north of the plant at a distance of about 2.0 km (Fig. 1). A complete view of the windward face of the Copithorne Ridge, the gas processing plant, and the behaviour of the cooling tower plume across the ridge can be seen from this trailer. It was necessary to use two cameras to view the entire scene, because the maximum angle of view of each camera is limited to 37°. Identical 16 mm Bolex Paillard

Model H-16 reflex movie cameras equipped with MRI Model 107-E intervalometers and Vario-Switar zoom lens were used. A small overlap of the field of view of both cameras was maintained in order to match the photographs taken from the two cameras; the SE trailer was used as the common object on both films. The filming rate was set at 90 seconds between frames with a common interval timer, which activated the two cameras to take pictures at the same moment. Kodachrome II film (25 ASA) and an exposure time of 1/33 of a second was used.

Because of reflection of sunlight from the snow covered ridge, the photographs taken during the winter of 1978 were overexposed for the majority of a sunny day. An automatic polarizer system developed by Haslett and Havlena (1973) was used during the next winter, and the quality of the photographs was substantially improved both in reducing the snow glare and in increasing the image contrast of the plume against the background sky.

Although the ice crystal plume from the cooling tower is clearly visible for at least the first kilometre on cold stable winter days with temperatures below -20°C, it is very seldom that the wind blows the plume towards the ridge on this type of day. Only four cases exist for the two winters and no marginal cases have been removed from the available data set (Lee, 1979); see Table 3. The film frame in each case that best depicts the time mean plume trajectory above the ridge was selected for analysis. The single camera technique of Halitsky (1961) was used to determine the shape of the plume outline, starting with the limits of visibility at the top and bottom edges of the plume in each photograph. The centreline is defined as the arithmetic mean distance between the top and bottom of the plume.

The plume outline for case 1 only is given here (Fig. 5) because the results for all four cases are very similar (Rowe, Lee, and Havlena, 1980). For case 1, it was not possible to see the bottom of the plume behind the ridge; the plume appeared to diffuse quite rapidly on this occasion. In all four cases, the plume rose vertically through an almost stagnant lower layer before it bent over into the wind direction in the upper layer. The plume overshot its equilibrium level slightly with a subsequent wave fluctuation, after this the plume leveled off and maintained an almost constant (effective stack) height upwind of the ridge. This plume height was only slightly greater than the height of the Copithorne Ridge, so that the influence of the ridge on the plume behaviour can be clearly seen.

For each set of photographs, the wind data taken at both the SE and the NE trailers have been analyzed in order to attempt to estimate the mean wind direction at the plume height. The results of these analyses showed that the wind directions detected at the SE trailer were more northerly than those obtained at the NE trailer. This phenemonon can be explained by the wind pattern near the SE trailer where the wind tends to move around and through the gap in the ridge. Luckily, all photographs were obtained when the plume moved across the ridge in the neighborhood of the NE trailer, which is the more interesting situation because the ridge is higher at that location. Therefore, the mean wind direction obtained from NE monitoring trailer alone is used to estimate the wind direction at the elevation of the plume centreline.

The wind direction for each case has been changed slightly by not more than 12 degrees from that monitored at the NE trailer so that the peak of the plume coincides with the ridge crest (Table 3). This change

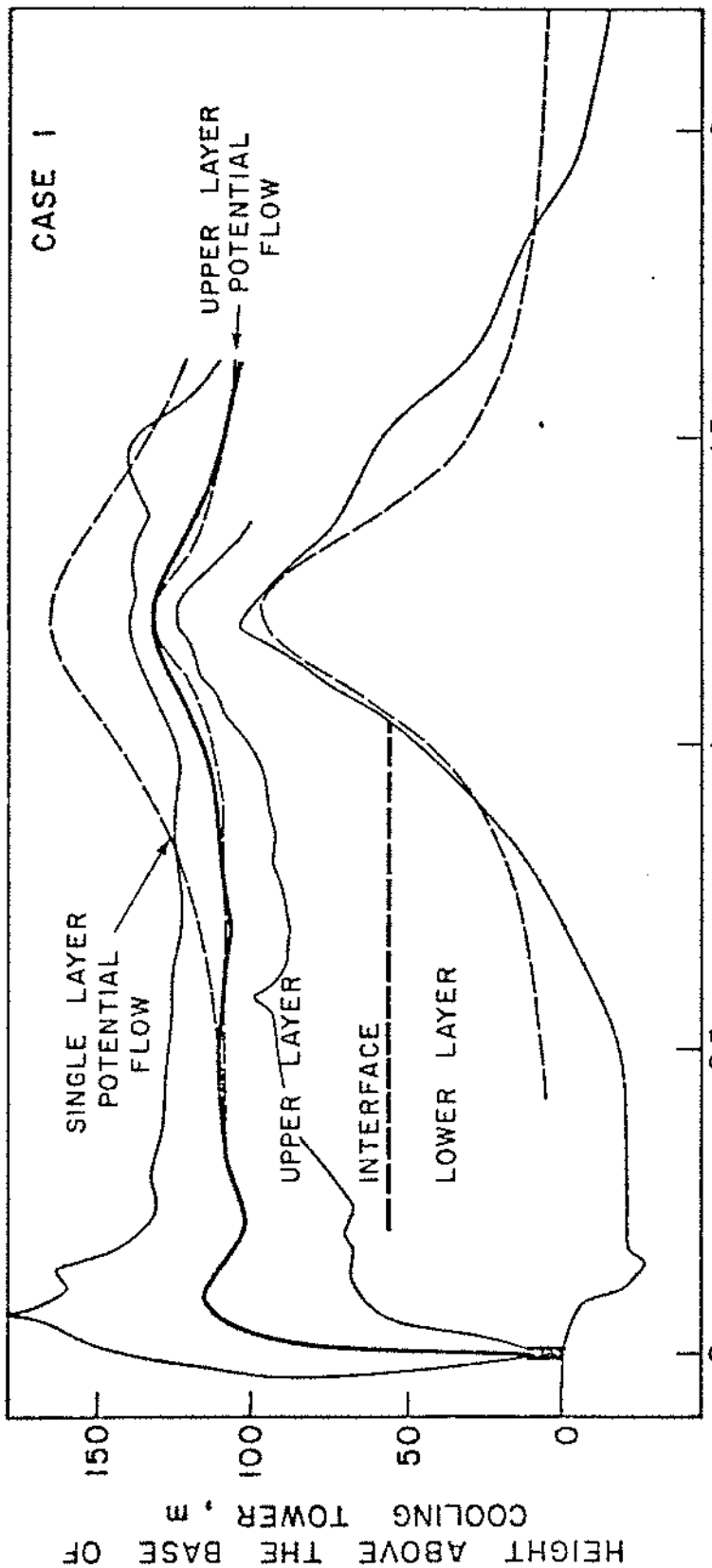

Fig. 5: Cooling tower plume outline and centreline trajectory. The potential flow streamlines for both the single-layer and the two-layer models are also shown. The dashed curve next to the ridge denotes the theoretical bell-shaped ridge.

of wind direction has been made in order that the experimental plume centreline trajectories can be compared with simple flow models, whose streamlines peak above the terrain crest. Discounting case 4, the wind direction angles had to be decreased by approximately 10 degrees. Using the wind direction monitored at the NE trailer, the plume peaks were located slightly downwind of the ridge crest. It is quite likely that the wind vane direction indicator was set with an error of at least 10 degrees and/or that there is a systematic wind directional shear above the ridge.

The corrected wind directions are all close to one another (Table 3); because of this an unexpected additional benefit was obtained in that the ridge contour for all four cases is more or less the same and therefore a single ridge shape could be used in all of the calculations. A bell-shaped ridge with a height h of 97 m and an aspect ratio of $L/h = 2$ has been used to represent the ridge shape for all cases. The plume outline, centerline trajectory, and the ridge shape for the corrected wind direction are shown in Fig. 5. The bell-shaped ridge (equation A14) is also drawn in this figure, and as can be seen it is a good approximation to the terrain shape. In some cases, $L/h = 2.5$ leads to a more reasonable approximation of the lower slopes of the ridge. However, in all cases $L/h = 2.0$ gives the best approximation to the upper part of the ridge, which is more influential in distorting the plume.

Single-layer flow models

The plume centreline trajectories obtained from this experiment are compared in this section with streamline prediction models that apply to single-layer flow for the calculation of streamline trajectories over

the two-dimensional ridge. The atmospheric boundary layer is assumed to have only one layer, and therefore all of the air flows over the ridge. Because the plume centreline trajectory is significantly distorted as it passes over the ridge, horizontal trajectory type models, such as the EPA Valley model (Burt and Slater, 1977), are excluded from this comparison. The models selected for this paper are all of the partial-height type, they are: potential flow (Appendix), half-height model (Egan, 1975), Alberta model (Alberta Department of the Environment, 1978), and LAPPES model (Slowik, Austin, and Pica, 1977). According to the Alberta model, the height z of a streamline with upstream elevation H_s is given by

$$z = \frac{H_s}{2} + \frac{1}{2}(H_s^2 + 4z_g^2)^{\frac{1}{2}} \qquad (3)$$

where z_g is the height of the terrain. The elevation of this steamline above the crest of a semi-circular cylinder has the same value as that for potential flow.

The calculations were made in such a way that the elevation of the upwind streamline matches the effective plume height for each case. As can be seen in Fig. 5, the single-layer potential flow model gives a very poor prediction of the plume centreline trajectory. The same result is true for all of the other models (Lee, 1979). However, compared to the other models, the LAPPES model gives a much better prediction; this is not surprising because this single-layer model was developed with an appreciation of the possibility of a two-layer flow regime.

Two-layer flow models

It is necessary to use a two-layer model to obtain reasonable agreement with the plume centreline. For simplicity, the two-layer model has

been applied to the lee side as well as to the windward side of the ridge. Even though this leads to good agreement on the downwind side for case 1, it should not be inferred that this approach provides in any way an adequate simplified description of the lee side flow; see, for example, Hunt and Snyder (1980).

Unfortunately, the environmental lapse rate was not measured because the critical importance of this variable was not recognised until the spring of 1979. However, the elevation of the interface between the two layers H_d can be determined for each model by making the theoretical streamlines in the upper layer fit the experimental plume centrelines at the crest of the ridge as well as at the effective plume height upwind of the ridge. Equation (A12) in the Appendix has been used to do this for the potential flow model. The values of H_d obtained for the potential flow model were substituted into equation (1) to calculate the Froude numbers given in Table 3. The LAPPES model has not been applied because it was specifically developed as a single-layer model for this type of situation. The order in which the other three models provide the best fit to the experimental data for all four cases is (Lee, 1979): 1st - potential flow; 2nd - half-height model; 3rd - Alberta model.

The lapse rates required to fit the two-layer model for the four cases have been compared to the lapse rate measured in the City of Calgary about 30 km east of the plant site (Leahey, 1977). Fig. 6 shows the median and 90 percentile values of the potential temperature gradient as observed over Calgary for the 25 worst air quality days for two winter seasons (1975 and 1976) as a function of time of day. Except for case 4, the lapse rates derived from the two-layer model are in good agreement with those

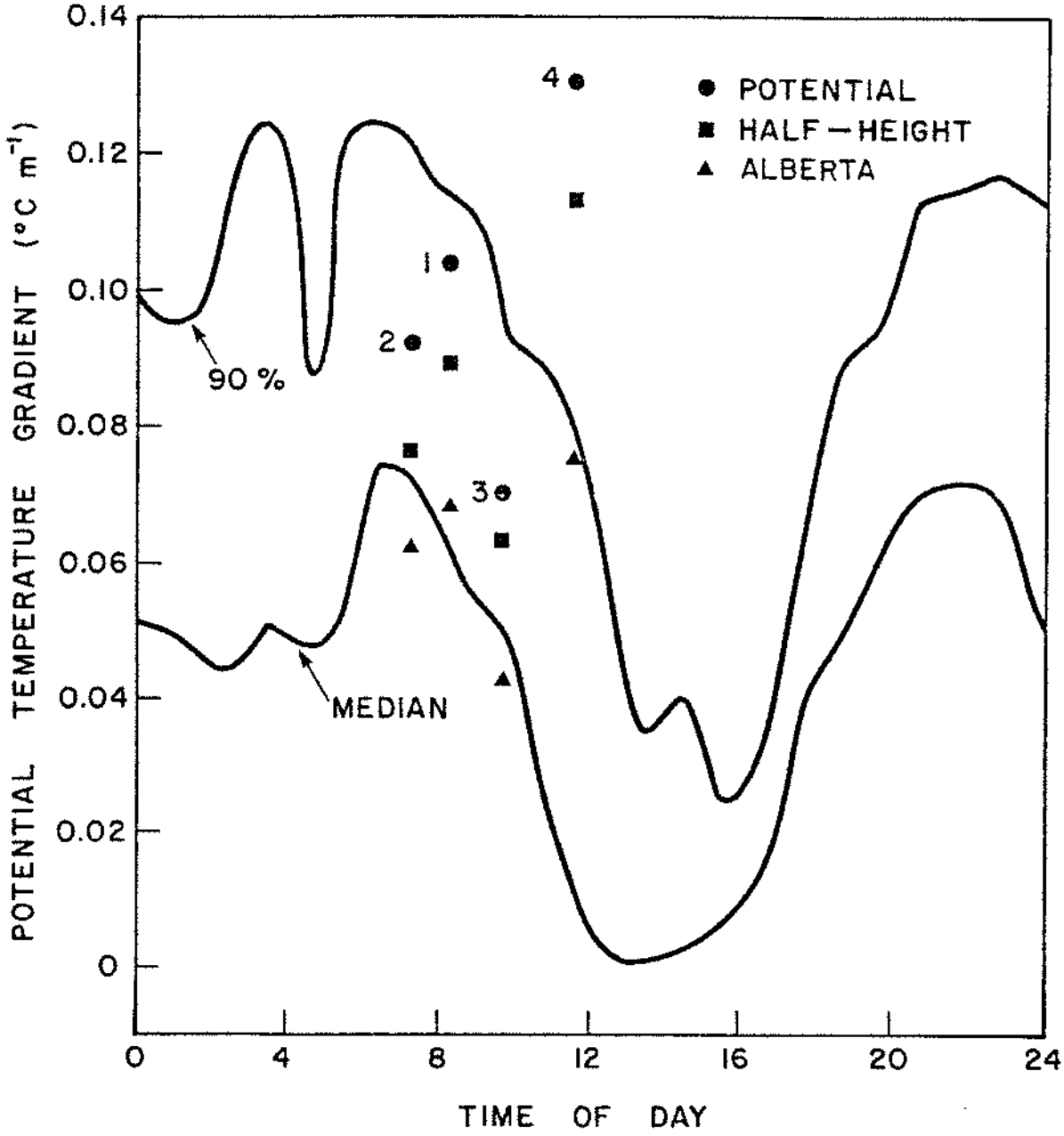

Fig. 6: 'Maximum' potential temperature gradient for the winter season.

observed in Calgary on very stable winter days.

Equation (1) has been used to determine the potential temperature gradients of the data points shown in Fig. 6. If equation (2) is used instead of equation (1) then the values of the potential temperature gradients would be four times larger, because the Brunt-Vaisala frequency is proportional to the square root of the potential temperature gradient (Appendix). The laboratory data of Hunt and Snyder (1980), which are reviewed in Section 1, show that when $F < 1$ the flow streamlines in the upper layer above a hill come much closer to its peak than those predicted by potential flow. It seems unlikely that the streamlines in the upper layer above the Copithorne Ridge would come closer to the crest than those given by the Alberta model. In which case, the potential temperature gradient would need to have the excessively large value of approximately 20°C/100 m to satisfy equation (2) due to Baines (1979).

Finally, it can be seen in Fig. 5 that for these very stable atmospheres the plume width above the ridge given by the distance between the edges is only about 20 m. These plumes are much narrower than those for a Pasquill-Gifford type F moderately stable atmosphere.

Table 3. Summary of the four occasions when the cooling tower plume was visible above the ridge.

Case	Date	Time (hours)	Wind at NE trailer (degrees)	Corrected direction (degrees)	Speed at NE trailer (m/s)	$\frac{U}{N}$ (m)	F
1	Feb. 1, 1978	0809	257	248	2.7	42.1	0.43
2	Feb. 16, 1979	0723	268	256	1.6	26.7	0.28
3	Feb. 17, 1979	0937	262	252	2.2	42.0	0.43
4	Feb. 24, 1979	1132	244	243	1.6	22.3	0.23

7. CONCLUSIONS

The data obtained from three different field experiments concerned with stable flow over and around a ridge are shown to be in good agreement with a simple two-layer model for the flow on the upwind side of a terrain feature. When the Froude number F is less than one ($F < 1$) the stable flow splits into two layers, the upper layer flows over the ridge whilst the lower layer flows around it. The streamlines in the layer that cross the ridge, whether it be the upper of two layers or a single layer, can be approximated by potential flow. It has been demonstrated previously that potential flow can also be used to model single layer neutral stability flow across this ridge (Leahey and Rowe, 1974).

The elevations of the interface between the two layers H_d deduced from these field data for this long reasonably two-dimensional ridge with a length-to-width ratio of about 5 are shown to be in much better agreement with laboratory data for axisymmetric hills (Snyder, Britter, and Hunt, 1979) rather than those for two-dimensional barriers with gaps (Baines, 1979).

It is concluded that the simple model discussed in this paper can be used to determine the plume centreline location for air pollution dispersion calculations on the windward side and on the top of terrain features for both stable and neutral atmospheres. However, the flow structure on the lee side of terrain obstacles is much more complicated and this simple model should not be applied on the downwind side.

Acknowledgements

The support and hard work at all times of the day and night of our research assistants Messrs. J. Boyle and A. Omar, and many others, is very gratefully acknowledged. Thanks are also due to the cooperative grant funding coordinators Drs. H.S. Sandhu and M.D. Winning for their encouragement and patience.

The smoke timelines experiment was supported by a Canadian NRC negotiated development grant to UNISUL (University of Calgary Interdisciplinary Sulphur Research Group) and by NRC operating grant (A6070). The plume photography and tetroon flights experiments were supported by a cooperative grant from the Alberta Environmental Research Trust and Shell Canada Resources Limited. This paper was written during the award of a Killam Resident Fellowship to R.D.R..

REFERENCES

Alberta Department of the Environment (1978) Guidelines for plume dispersion calculations. Edmonton, Alberta, Canada.

Baines P.G. (1977) Upstream influence and Long's model in stratified flows. *J. Fluid Mech.* 82, 147-159.

Baines P.G. (1979) Observations of stratified flow past three-dimensional barriers. *J. Geophys. Res.* 84, 7834-7838.

Benjamin S.F. (1976) A photogrammetric flow visualization technique used during a field experiment to study air motions around a ridge of high ground. UNISUL Report, Univ. of Calgary, Alberta.

Benjamin S.F. Havlena J.J. and Rowe R.D. (1978) Field investigations of the dispersion of pollution across a ridge. Proceedings of the 9th International Technical Meeting on Air Pollution Modelling and its Application, Toronto, 46-55.

Benjamin S.F. and Rowe R.D. (1979) Analysis of SO_2 data on a ridge. 13th Congress of the Canadian Meteorological and Oceanographic Society, Victoria.

Brighton P.W.M. (1978) Strongly stratified flow past three-dimensional obstacles. *Q. Jl. R. Met. Soc.* 104, 289-307.

Burt E.W. and Slater H.H. (1977) Evaluation of the valley model. Proceedings of AMS-APCA Joint Conference on Applications of Air Pollution Meteorology, Salt Lake City, 192-195.

Chung K.P. (1979) Tetroon flights across a two-dimensional ridge under stable atmospheric conditions. M.Sc. thesis, Univ. of Calgary, Alberta.

Drazin P.G. (1961) On the steady flow of a fluid of variable density past an obstacle. *Tellus* 13, 239-251.

Egan B.A. (1975) Turbulent diffusion in complex terrain. Chapter 4 in Lectures on Air Pollution and Environmental Impact Assessment, American Meteorological Society, Boston, 112-135.

Halitsky J. (1961) Single-camera measurement of smoke plumes. *Int. J. Air Water Pollut.* 4, 185-198.

Haslett J.M. and Havlena J.J. (1973) A remote pollution monitor. *J. Physics E: Scientific Instruments* 6, 98-100.

Hunt J.C.R. Puttock J.S. and Snyder W.H. (1979) Turbulent diffusion from a point source in stratified and neutral flows around a three-dimensional hill - Part 1. Diffusion equation analysis. *Atmospheric Environment* 13, 1227-1239.

Hunt J.C.R. and Snyder W.H. (1980) Experiments on stably and neutrally stratified flow over a model three-dimensional hill. *J. Fluid Mech.* 96, 671-704.

Leahey D.M. and Rowe R.D. (1974) Observational studies of atmospheric diffusion processes over irregular terrain. Proceedings of the 67th Annual APCA Meeting, Denver, paper no. 74-67.

Leahey D.M. (1977) A preliminary study of the effects of the Chinook on the air pollution levels in Calgary. Western Research and Development Ltd. Report, Calgary, Alberta.

Lee C.Z. (1979) Plume trajectories across a ridge under stable atmospheric conditions. M.Sc. thesis, Univ. of Calgary, Alberta.

Rowe R.D. (1980) A simple two-layer model for stable air flow across terrain features. Proceedings of the 2nd Joint Conference on Applications of Air Pollution Meteorology, New Orleans, 559-566.

Rowe R.D. Lee C.Z. and Havlena J.J. (1980) The elevation of stable atmosphere plumes above a ridge. Proceedings of the 73rd Annual APCA Meeting, Montreal, paper no. 80-55.5.

Scorer R.S. (1968) *Air Pollution*, Pergamon Press.

Scorer R.S. (1978) *Environmental Aerodynamics*, Ellis Horwood Ltd.

Seinfeld J.H. (1975) *Air Pollution - Physical and Chemical Fundamentals*, McGraw-Hill Book Company.

Sheppard P.A. (1956) Airflow over mountains. *Q. Jl. R. Met. Soc.* 82, 528-529.

Slowik A.A. Austin J.M. and Pica G.N. (1977) Plume dispersion modeling in complex terrain under stable atmospheric conditions. Proceedings of the 70th Annual APCA Meeting, Toronto, paper no. 77-29.1.

Snyder W.H. Britter R.E. and Hunt J.C.R. (1979) A modeling study of the flow structure and plume impingement on a three dimensional hill in stably stratified flow. Proceedings of the 5th International Conference on Wind Engineering, Fort Collins, Pergamon Press.

APPENDIX

Determination of interface elevation, H_d

Consider an air parcel moving horizontally with a speed U well upstream of a terrain obstacle at an elevation H_s above the base of the obstacle, as shown in Fig. A1. The parcel is displaced in the vertical direction z as it surmounts the obstacle; distance along its streamline is given by s. Assuming inviscid flow, the application of Newton's Second Law yields

$$q \frac{dq}{ds} = g\left(\frac{\rho_a - \rho}{\rho}\right) \frac{dz}{ds} \tag{A1}$$

where q = parcel speed,

ρ = density,

and the subscript a denotes the ambient air. Air behaves as an ideal gas, and the air parcel is assumed to cool adiabatically, so

$$\frac{\rho_a - \rho}{\rho} = \frac{T - T_a}{T_a} = \frac{\Lambda - \Gamma}{T_a} (z - H_s) \tag{A2}$$

where $T = T_s - \Gamma(z - H_s)$,

$T_a = T_s - \Lambda(z - H_s)$,

T_s = temperature at elevation H_s,

Γ = adiabatic lapse rate,

Λ = ambient lapse rate.

It can be shown (see, for example, Seinfeld, 1975) that

$$\frac{\Lambda - \Gamma}{T_a} = -\frac{1}{\theta} \frac{d\theta}{dz} \simeq -\frac{1}{T_s} \frac{d\theta}{dz} \tag{A3}$$

where θ = potential temperature.

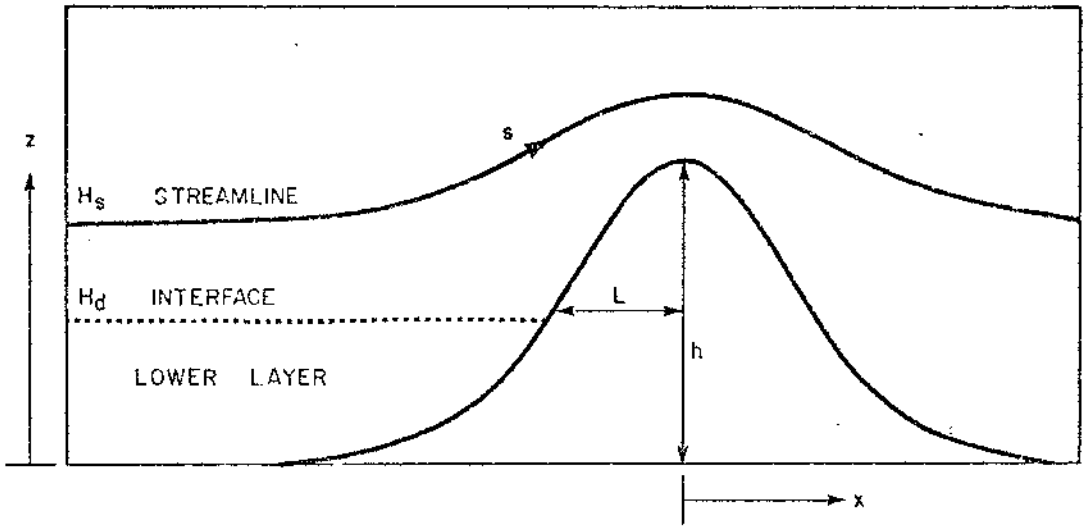

Fig. A1. A schematic diagram of a stable flow streamline in the upper layer across a terrain obstacle.

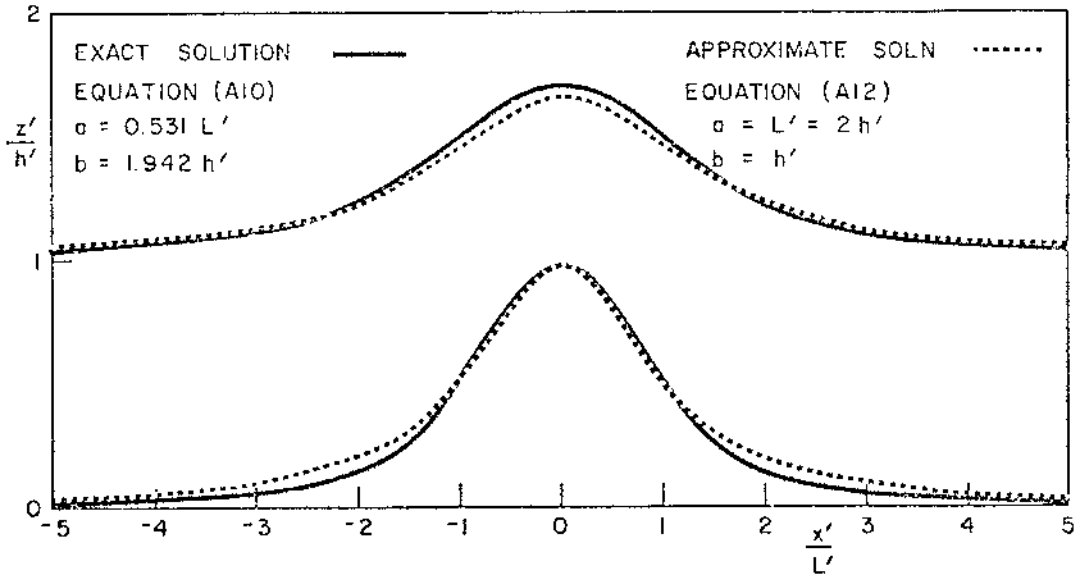

Fig. A2. Exact and approximate potential flow solutions for a bell shaped ridge.

The Brunt-Vaisala frequency is given by

$$N = \left(\frac{g}{T_s} \frac{d\theta}{dz}\right)^{\frac{1}{2}}$$

Therefore, equation (A1) can be written

$$q \frac{dq}{ds} = -N^2(z - H_s)\, dz \tag{A4}$$

Integration of equation (A4) yields

$$U^2 - q^2 = N^2(z - H_s)^2 \tag{A5}$$

The dividing streamline between the two layers has an upstream elevation H_d such that $q = 0$ when $z = h$, the elevation of the terrain obstacle. Therefore, the vertical distance down from the crest of the terrain to the interface between the two layers is given by

$$h - H_d = \frac{U}{N} \tag{A6}$$

The Froude number for stable flow with a characteristic length scale h is given by

$$F = \frac{U}{Nh}$$

and equation (A6) can be written

$$H_d = h(1 - F) \tag{A7}$$

Potential flow equation

A typical potential flow streamline path across a two-dimensional symmetrical ridge is shown in Fig. A1, the upstream elevation of this streamline above the base of the ridge is given by H_s. For the flow in the upper layer that passes over a ridge, it is necessary to consider values relative to the interface between the two layers which are denoted by a prime,

e.g. $H'_s = H_s - H_d$. It can easily be verified that the following stream function ψ satisfies Laplace's equation

$$\psi = U\left[z' - \frac{ab(a + z')}{(a + z')^2 + x^2}\right] \tag{A8}$$

where a and b are constants, x is downwind distance relative to the ridge crest, and U is the upstream wind speed which has a constant value independent of elevation. Therefore, at a long distance upwind of the ridge

$$\psi = UH'_s \tag{A9}$$

Combining equations (A8) and (A9) yields

$$z' = H'_s + \frac{ab(a + z')}{(a + z')^2 + x^2} \tag{A10}$$

The ground level contour above the interface z'_g is obtained by setting $H'_s = 0$

$$z'_g = \frac{ab(a + z'_g)}{(a + z'_g)^2 + x^2} \tag{A11}$$

Unique values can be obtained for a and b if the height h' and the length between the half-height positions $2L'$ for a symmetrical two-dimensional terrain obstacle are specified.

For a broad ridge $L' >> h'$, the elevation perturbation of a streamline is small and $z' \approx H'_s$ so that z' can be approximated by

$$z' = H'_s + \frac{ab(a + H'_s)}{(a + H'_s)^2 + x^2} \tag{A12}$$

At the level of the dividing streamline between the two layers $H'_s = 0$, and equation (A12) reduces to

$$z'_g = \frac{a^2 b}{a^2 + x^2} \tag{A13}$$

In this case, it is easy to show that $b = h'$ and $a = L'$, therefore

$$z'_g = \frac{L'^2 h'}{L'^2 + x^2} \tag{A14}$$

which is the ground profile of a bell-shaped ridge.

The accuracy of the approximate solution (equation (A12)) may be determined by comparing the streamlines predicted by the exact solution (equation (A10)) with those predicted by the approximate solution. As an example, the predictions for the streamlines with an upstream elevation equal to the ridge height h' for a ridge with an aspect ratio $L'/h' = 2$ are shown in Fig. A2. It can be seen that there is very little difference between the two ground level profiles (equations (A11) and (A13)) or between the two streamlines. A maximum difference of only 9.5% between the values of z' is found at the ridge crest. For this reason, the approximate solution is used to determine the potential flow streamlines in the upper layer that traverses the ridge.